J|A|C|S
ARTICLES
Published on Web 11/08/2006

Topological Control in Heterometallic Metal−Organic Frameworks by Anion Templating and Metalloligand Design

Sara R. Halper, Loi Do, Jay R. Stork, and Seth M. Cohen*

Contribution from the Department of Chemistry and Biochemistry, University of California, San Diego, La Jolla, California, 92093-0358

Received July 5, 2006; E-mail: scohen@ucsd.edu

Abstract: Several new heterometallic metal−organic frameworks (MOFs) based on tris(dipyrrinato) metalloligands and Ag^+ salts are reported. MOFs were prepared systematically to examine the effects of the core metal ion, counteranion, and ligand structure on the topology of the resultant network. The effect of the metal ion (Fe^{3+} vs Co^{3+}) on MOF structure was generally found to be negligible, thereby permitting the facile synthesis of trimetallic Fe/Co/Ag networks. The choice of anion (e.g., silver salt) was found to have a pronounced effect on the MOF topology. Networks prepared with salts of AgO_3SCF_3 and $AgBF_4$ reliably formed three-dimensional (10,3) nets, whereas use of $AgPF_6$ and $AgSbF_6$ produced two-dimensional (6,3) honeycomb nets. The topology generated upon formation of the MOF was found to be robust in certain cases, as demonstrated by anion-exchange experiments. Anion exchange was confirmed by X-ray crystallography in a rare set of apparent single-crystal-to-single-crystal transformations. The data presented here strongly suggest that the coordinative ability of the anion does not play a significant role in the observed templating effect. Finally, changes in the length of the tris(dipyrrinato) metalloligand were found to override the anion templating effect, resulting exclusively in two-dimensional (6,3) nets. These studies provide a basis for the rational design of MOF topologies by choice of ligand structure and anion templating effects. Furthermore, the results demonstrate the ability of carefully designed metalloligands to generate MOFs of structure strikingly similar to that of their organic counterparts.

Introduction

At the forefront of modern materials chemistry and nanoscience is the design and synthesis of solid-state compounds known as metal−organic frameworks (MOFs).[1−4] The compounds are tailorable, low-density solids with tremendous promise for use in gas storage, molecular sensing, and other materials applications.[5] Many robust, highly porous MOFs have been prepared that may be particularly useful in gas storage and separations.[6−8] A continuing challenge in the field of MOFs is the ability to reliably predict the topology of a MOF based solely on the structure of the individual precursors. Although a number of MOFs have been prepared and certain structural motifs are found to be most common,[9,10] predicting the structure of a framework de novo remains elusive. In addition to structure prediction, another major challenge in the field is the introduction of complex functionality (e.g., catalysis, luminescence, etc.) into MOF assemblies.[5,11−13] Efforts to introduce more complex functionality include modification of the ligand structure and forcing sites of unsaturation or labile solvent coordination at the metal nodes. Among the most attractive strategies for introducing new functionality is the use of "metalloligands", that is coordination complexes as building blocks in lieu of simple organic ligands.[13] Such metalloligands have been shown to have the ability to introduce rich spectroscopic and magnetic features to MOFs,[14−17] in addition to providing sites for introducing unsaturated metal centers.[18−22]

(1) Eddaoudi, M.; Moler, D. B.; Li, H.; Chen, B.; Reineke, T. M.; O'Keeffe, M.; Yaghi, O. M. *Acc. Chem. Res.* **2001**, *34*, 319−330.
(2) Holliday, B. J.; Mirkin, C. A. *Angew. Chem., Int. Ed.* **2001**, *40*, 2022−2043.
(3) O'Keeffe, M.; Yaghi, O. M. *J. Solid State Chem.* **2005**, *178*, V−VI.
(4) Moulton, B.; Zaworotko, M. J. *Chem. Rev.* **2001**, *101*, 1629−1658.
(5) Hupp, J. T.; Poeppelmeier, K. R. *Science* **2005**, *309*, 2008−2009.
(6) Rosi, N. L.; Eckert, J.; Eddaoudi, M.; Vodak, D. T.; Kim, J.; O'Keeffe, M.; Yaghi, O. M. *Science* **2003**, *300*, 1127−1129.
(7) Chae, H. K.; Siberio-Pérez, D. Y.; Kim, J.; Go, Y.; Eddaoudi, M.; Matzger, A. J.; O'Keeffe, M.; Yaghi, O. M. *Nature* **2004**, *427*, 523−527.
(8) Bennett, M. V.; Beauvais, L. G.; Shores, M. P.; Long, J. R. *J. Am. Chem. Soc.* **2001**, *123*, 8022−8032.
(9) Ohrstrom, L.; Larsson, K. *Molecule-Based Materials: The Structural Network Approach*; Elsevier: Amsterdam, 2005; p 314.
(10) Ockwig, N. W.; Delgado-Friedrichs, O.; O'Keeffe, M.; Yaghi, O. M. *Acc. Chem. Res.* **2005**, *38*, 176−182.
(11) Wu, C. D.; Hu, A.; Zhang, L.; Lin, W. B. *J. Am. Chem. Soc.* **2005**, *127*, 8940−8941.
(12) Wu, C. D.; Ngo, H. L.; Lin, W. B. *Chem. Commun.* **2004**, 1588−1589.
(13) Kitagawa, S.; Kitaura, R.; Noro, S. *Angew. Chem., Int. Ed.* **2004**, *43*, 2334−2375.
(14) Decurtins, S.; Schmalle, H. W.; Oswald, H. R.; Linden, A.; Ensling, J.; Gutlich, P.; Hauser, A. *Inorg. Chim. Acta* **1994**, *216*, 65−73.
(15) Decurtins, S.; Schmalle, H. W.; Pellaux, R.; Schneuwly, P.; Hauser, A. *Inorg. Chem.* **1996**, *35*, 1451−1460.
(16) Decurtins, S.; Schmalle, H. W.; Schneuwly, P.; Ensling, J.; Gütlich, P. *J. Am. Chem. Soc.* **1994**, *116*, 9521−9528.
(17) Sharma, C. V. K.; Broker, G. A.; Huddleston, J. G.; Baldwin, J. W.; Metzger, R. M.; Rogers, R. D. *J. Am. Chem. Soc.* **1999**, *121*, 1137−1144.
(18) Smithenry, D. W.; Suslick, K. S. *J. Porphyrins Phthalocyanines* **2004**, *8*, 182−190.
(19) Smithenry, D. W.; Wilson, S. R.; Suslick, K. S. *Inorg. Chem.* **2003**, *42*, 7719−7721.
(20) Suslick, K. S.; Bhyrappa, P.; Chou, J. H.; Kosal, M. E.; Nakagaki, S.; Smithenry, D. W.; Wilson, S. R. *Acc. Chem. Res.* **2005**, *38*, 283−291.
(21) Kitaura, R.; Onoyama, G.; Sakamoto, H.; Matsuda, R.; Noro, S.; Kitagawa, S. *Angew. Chem., Int. Ed.* **2004**, *43*, 2684−2687.
(22) Chen, B. L.; Fronczek, F. R.; Maverick, A. W. *Inorg. Chem.* **2004**, *43*, 8209−8211.

To date, most metalloligands have utilized the same general donor groups found in many organic ligands used in MOFs (e.g., carboxylate, nitrile, and pyridyl ligands), but have not necessarily reproduced the size and shape of the organic ligands used in MOF synthesis. The potential advantage of replicating both the donor atoms and overall structure of an organic ligand in a metalloligand is the possibility of generating specific, i.e., predictable, MOF topologies by prior knowledge of the analogous organic ligand MOF. For example, if a specific MOF is found to have structural properties (e.g., microporosity, pore shape, thermal stability, etc.) desirable for a specific application, then designing a metalloligand that reproduces that structure with high fidelity would allow for retention of the framework topology while introducing new functionality that originates from the metalloligand metal center. The enormous number of MOF structures derived from organic ligands described to date provides a general strategy for the preparation of MOFs of a selected topology and functionality based on analogous metalloligand precursors. Realization of this goal is the focus of the studies detailed herein.

Recently, we have described several dipyrromethene (dipyrrinato, dipyrrin) coordination complexes[23,24] that generally reproduce the structures found in a class of organic ligand MOFs reported by Lee, Moore, and co-workers.[25−28] These dipyrrinato, metalloligand-based MOFs generate materials with strong optical absorptions and show potential for the synthesis of chiral MOFs derived from the Δ/Λ configuration at a tris(chelate) metal center.[24] On the basis of these early findings, we report here a more comprehensive, systematic investigation of these dipyrrin-based metalloligand systems, describing 14 new, crystallographically characterized MOF structures. A pronounced anion templating is reported, which permits control over two- (2D) versus three-dimensional (3D) framework structures. The consequence of changes in metalloligand composition on MOF structure have also been studied and are found to closely parallel those observed in analogous three-fold symmetric organic ligand systems. All in all, the findings here show that tris(dipyrrinato) metal complexes appended with peripheral binding groups are a versatile class of metalloligands for preparing a variety of functionalized MOF structures.

Experimental

General. Unless otherwise noted, starting materials were obtained from commercial suppliers and used without further purification. [Co(4-pyrdpm)$_3$] and [Fe(4-pyrdpm)$_3$] (4-pyrdpm = 5-(4-pyridyl)-4,6-dipyrrinato) were prepared as previously described.[23] Mass spectrometry was performed at the University of California, San Diego, Mass Spectrometry Facility in the Department of Chemistry and Biochemistry. A ThermoFinnigan LCQ-DECA mass spectrometer was used for ESI or APCI analysis, and the data were analyzed using the Xcalibur software suite. A ThermoFinnigan MAT 900XL mass spectrometer was used to acquire the data for the high-resolution mass spectra (HRMS). Infrared spectra were collected on either a Mattson Research Series or an Avatar 360 (Thermo Nicolet) FT-IR instrument (using KBr pellets or NaCl plates) at the Department of Chemistry and Biochemistry, University of California, San Diego. ^{1}H/^{13}C/^{19}F NMR spectra were recorded on Varian FT-NMR spectrometers at the Department of Chemistry and Biochemistry, University of California, San Diego. UV−visible spectra were recorded in CH_2Cl_2 using a Perkin-Elmer Lambda 25 spectrophotometer with the UVWinLab 4.2.0.0230 software package.

[Co(4-pyrdpm)$_3$AgBF$_4$] (MOF-Co/AgBF$_4$-1). In the following order, 1 equiv of a benzene solution containing 3.5 mM [Co(4-pyrdpm)$_3$], neat benzene, and 1 equiv of a benzene solution containing 3.5 mM $AgBF_4$ were placed into a glass test tube.[23] Different solution volumes were used in order to obtain mixtures containing from ∼0.22 to 1.3 mM of each reactant. At all concentrations, a precipitate formed immediately upon addition of $AgBF_4$, which was dissolved by addition of ∼1.0 mL of acetonitrile. The solutions were stored in the dark and left to slowly evaporate. Orange crystals grew from all solutions after ∼7−15 days. For a solution containing 1.3 mM [Co(4-pyrdpm)$_3$], 1.3 mM $AgBF_4$, and 1.0 mL of acetonitrile (total volume 4.0 mL) the isolated yield of crystalline material was 1.7 mg (36%). IR (KBr pellet): ν 1540, 1380, 1345, 1247, 1032, 994 cm^{-1}.

[Fe(4-pyrdpm)$_3$AgOTf] (MOF-Fe/AgOTf-1). The same procedure was used as in the synthesis of MOF-Co/AgBF$_4$-1. For a solution containing 2.6 mM [Fe(4-pyrdpm)$_3$], 2.6 mM AgOTf, and 1.0 mL of acetonitrile (total volume 4.0 mL) the isolated yield of crystalline material was 4.6 mg (32%). IR (KBr pellet): ν 1561, 1379, 1336, 1242, 1039, 996 cm^{-1}.

[Co(4-pyrdpm)$_3$AgPF$_6$] (MOF-Co/AgPF$_6$-1). The same procedure was used as in the synthesis of MOF-Co/AgBF$_4$-1. For a solution containing 1.7 mM [Co(4-pyrdpm)$_3$], 1.7 mM $AgPF_6$, and 1.0 mL of acetonitrile (total volume 4.0 mL) the isolated yield of crystalline material was 4.8 mg (80%). IR (KBr pellet): ν 1561, 1382, 1345, 1247, 1034, 996, 840, 802 cm^{-1}.

[Fe(4-pyrdpm)$_3$AgPF$_6$] (MOF-Fe/AgPF$_6$-1). The same procedure was used as in the synthesis of MOF-Co/AgBF$_4$-1. For a solution containing 1.7 mM [Fe(4-pyrdpm)$_3$], 1.7 mM $AgPF_6$, and 1.0 mL of acetonitrile (total volume 4.0 mL) the isolated yield of crystalline material was 3.9 mg (65%). IR (KBr pellet): ν 1550, 1379, 1336, 1242, 1039, 995, 840, 811 cm^{-1}.

[Co(4-pyrdpm)$_3$AgSbF$_6$] (MOF-Co/AgSbF$_6$-1). The same procedure was used as in the synthesis of MOF-Co/AgBF$_4$-1. For a solution containing 0.43 mM [Co(4-pyrdpm)$_3$], 0.43 mM $AgSbF_6$, and 1.0 mL of acetonitrile (total volume 4.0 mL) the isolated yield of crystalline material was 0.9 mg (49%). IR (KBr pellet): ν 1562, 1380, 1345, 1254, 1032, 995 cm^{-1}.

[Fe(4-pyrdpm)$_3$AgSbF$_6$] (MOF-Fe/AgSbF$_6$-1). The same procedure was used as in the synthesis of MOF-Co/AgBF$_4$-1. For a solution containing 1.4 mM [Fe(4-pyrdpm)$_3$], 1.4 mM $AgSbF_6$, and 1.0 mL of acetonitrile (total volume 5.6 mL) the isolated yield of crystalline material was 3.4 mg (32%). IR (KBr pellet): ν 1561, 1379, 1336, 1242, 1040, 996, 769, 657 cm^{-1}.

[Co(4-pyrdpm)$_3$Fe(4-pyrdpm)$_3$(AgOTf)$_2$] (MOF-CoFe/AgOTf-1). In the following order, 1 equiv of a benzene solution containing 3.5 mM [Fe(4-pyrdpm)$_3$] and 3.5 mM [Co(4-pyrdpm)$_3$], neat benzene, and 1 equiv of a benzene solution containing 7.0 mM AgOTf were placed into a glass test tube. Different solution volumes were used in order to obtain mixtures containing from ∼0.22 to 1.3 mM of each reactant. At all concentrations, a precipitate formed immediately upon addition of AgOTf, which was dissolved by addition of ∼1.0 mL of acetonitrile. The solutions were stored in the dark and left to slowly evaporate. For a solution containing 0.88 mM [Fe(4-pyrdpm)$_3$], 0.88 mM [Co(4-pyrdpm)$_3$], 1.75 mM AgOTf, and 1.0 mL of acetonitrile (total volume 4.0 mL) the isolated yield of crystalline material was 2.8 mg (42%). IR (KBr pellet): ν 1563, 1381, 1346, 1252, 1031, 995 cm^{-1}.

[Co(4-pyrdpm)$_3$Fe(4-pyrdpm)$_3$(AgBF$_4$)$_2$] (MOF-CoFe/AgBF$_4$-1). The same procedure was used as in the synthesis of MOF-CoFe/AgOTf-1. For a solution containing 0.88 mM [Fe(4-pyrdpm)$_3$], 0.88 mM [Co-

(23) Halper, S. R.; Cohen, S. M. *Inorg. Chem.* **2005**, *44*, 486−488.
(24) Murphy, D. L.; Malachowski, M. R.; Campana, C. F.; Cohen, S. M. *Chem. Commun.* **2005**, 5506−5508.
(25) Kiang, Y.-H.; Lee, S.; Xu, Z.; Choe, W.; Gardner, G. B. *Adv. Mater.* **2000**, *12*, 767−770.
(26) Kiang, Y.-H.; Gardner, G. B.; Lee, S.; Xu, Z.; Lobkovsky, E. B. *J. Am. Chem. Soc.* **1999**, *121*, 8204−8215.
(27) Choe, W.; Kiang, Y.-H.; Xu, Z.; Lee, S. *Chem. Mater.* **1999**, *11*, 1776−1783.
(28) Xu, Z.; Kiang, Y.-H.; Lee, S.; Lobkovsky, E. B.; Emmott, N. *J. Am. Chem. Soc.* **2000**, *122*, 8376−8391.

(4-pyrdpm)$_3$], 1.75 mM $AgBF_4$, and 1.0 mL of acetonitrile (total volume 4.0 mL) the isolated yield of crystalline material was 5.5 mg (87%). IR (KBr pellet): ν 1562, 1383, 1346, 1245, 1084, 1040, 996 cm^{-1}.

[Co(4-quindpm)$_3$]. The same procedure was used as for the preparation of [Co(4-pyrdpm)$_3$],[23] but starting from 5-(4-quinolyl)-dipyrromethane[29] (100 mg, 0.37 mmol). Yield: 48% (51 mg). ^{1}H NMR ($CDCl_3$ 300 MHz, 25 °C): δ 6.35−6.65 (m, 6H), 7.42 (t, 1H), 7.50 (t, 1H), 7.67 (t, 1H), 7.72 (d, 1H), 8.20 (d, 1H), 9.03 (d, 1H). GC-EIMS: *m*/*z* 870.1 [M + H]$^+$. HR-EIMS Calcd for $C_{54}H_{37}N_9Co$: 870.2498. Found: 870.2492. λ_{max} (CH_2Cl_2) = 267, 295, 315, 405, 471, 511 nm. IR (film from CH_2Cl_2): ν 1557, 1378, 1360, 1249, 1039, 1023, 1001, 826 cm^{-1}.

[Fe(4-quindpm)$_3$]. The same procedure was used as for the preparation of [Fe(4-pyrdpm)$_3$],[23] but starting from 5-(4-quinolyl)-dipyrromethane[29] (250 mg, 0.92 mmol). Yield: 41% (110 mg). GC-EIMS: *m*/*z* 867.0 [M + H]$^+$. HR-EIMS Calcd for $C_{54}H3_7N_9Fe$: 867.2516. Found: 867.2519. λ_{max} (CH_2Cl_2) = 265, 292, 315, 446, 496 (shoulder) nm. IR (film from CH_2Cl_2): ν 1554, 1380, 1336, 1244, 1039, 996, 825 cm^{-1}.

[Fe(4-quindpm)$_3$AgOTf] (MOF-Fe/AgOTf-3). The same procedure was used as in the synthesis of MOF-Co/$AgBF_4$-1. For a solution containing 0.75 mM [Fe(4-quindpm)$_3$], 0.75 mM AgOTf, and 1.0 mL of acetonitrile (total volume 4.0 mL) the isolated yield of crystalline material was 1.3 mg (38%). IR (KBr pellet): ν 1560, 1554, 1400, 1377, 1242, 1038, 995 cm^{-1}.

[4-(Pyridin-4-ylethynyl)benzaldehyde]. A mixture of 4-(ethynyl)-benzaldehyde (0.33 g, 2.5 mmol), 4-bromopyridine hydrochloride (0.64 g, 3.3 mmol), $Pd(PPh_3)_2Cl_2$ (89 mg, 0.13 mmol), CuI (24 mg, 0.13 mmol), and 25 mL of dry diethylamine was stirred under a nitrogen atmosphere for 24 h. The reaction mixture was subsequently evaporated to dryness and then redissolved in 75 mL of CH_2Cl_2. The organic solution was washed with 75 mL of H_2O and 75 mL of brine and was then dried over $MgSO_4$. The CH_2Cl_2 was evaporated to dryness, and the resulting residue was purified by column chromatography (SiO_2; CH_2Cl_2/1% MeOH) to afford the product as a yellow solid. Yield: 58% (0.31 g). GC−EIMS: *m*/*z* 207.1 [M]$^+$. ^{1}H NMR ($CDCl_3$ 400 MHz, 25 °C): δ 7.27 (d, 2H, J = 6.0 Hz), 7.55 (d, 2H, J = 8.4 Hz), 7.74 (d, 2H, J = 8.4 Hz), 8.51 (d, 2H, J = 4.0 Hz), 9.98 (s, 1H, CHO) ppm. ^{13}C NMR ($CDCl_3$ 100 MHz, 25 °C): δ 89.7, 92.2, 125.1, 127.6, 129.1, 130.1, 131.9, 135.6, 149.3, 190.6 ppm.

[5-(4-Pyridin-4-ylethynylphenyl)dipyrromethane]. The same procedure was used as in the synthesis of 5-(4-pyridyl)dipyrromethane,[23,30] but starting from [4-(pyridin-4-ylethynyl)benzaldehyde] (0.31 g, 1.5 mmol). The product was isolated as a pale-yellow solid. Yield: 40% (0.19 g). ESI-MS: *m*/*z* 324.12 [M + H]$^+$, 258.23 [M − pyrrole]$^+$. ^{1}H NMR ($CDCl_3$ 400 MHz, 25 °C): δ 5.50 (s, 1H), 5.90 (m, 2H), 6.17 (m, 2H), 6.72 (m, 2H), 7.23 (d, 2H, J = 8.0 Hz), 7.37 (d, 2H, J = 6.0 Hz), 7.49 (d, 2H, J = 8.4 Hz), 8.07 (bs, 2H, NH), 8.57 (d, 2H, J = 6.4 Hz). ^{13}C NMR ($CDCl_3$ 100 MHz, 25 °C): δ 43.9, 86.6, 93.8, 107.3, 108.4, 117.4, 120.5, 125.4, 128.4, 131.3, 131.6, 132.0, 143.3, 149.5 ppm.

[Co(4-papyrdpm)$_3$]. The same procedure was used as in the synthesis of [Co(4-pyrdpm)$_3$],[23] but starting from 5-(4-pyridin-4-ylethynylphenyl)dipyrromethane (0.50 g, 1.55 mmol). Yield: 38% (0.20 g). ESI-MS: *m*/*z* 1020.08 [M + H]$^+$. HR-FABMS Calcd for $C_{66}H_{42}N_9Co$: 1020.2968. Found: 1020.2957. ^{1}H NMR ($CDCl_3$ 400 MHz, 25 °C): δ 6.36 (m, 6H), 6.43 (s, 6H), 6.72 (m, 6H), 7.41 (d, 6H, J = 5.6 Hz), 7.48 (d, 6H, J = 8.0 Hz), 7.62 (d, 2H, J = 8.4 Hz), 8.62 ppm (d, 6H, J = 5.2 Hz). ^{13}C NMR ($CDCl_3$ 100 MHz, 25 °C): δ 87.6, 93.3, 118.9, 122.2, 125.4, 130.3, 130.6, 131.0, 132.7, 135.0, 138.6, 144.8, 149.5, 151.7 ppm. λ_{max} (CH_2Cl_2) = 228, 279, 293, 335, 398, 469, 506 nm. IR (KBr pellet): ν 1560, 1379, 1344, 1248, 1041, 1029, 998, 812 cm^{-1}.

(29) Halper, S. R.; Cohen, S. M. *Inorg. Chem.* **2005**, *44*, 4139−4141.
(30) Halper, S. R.; Malachowski, M. R.; Delaney, H. M.; Cohen, S. M. *Inorg. Chem.* **2004**, *43*, 1242−1249.

[Co(4-papyrdpm)$_3$AgOTf] (MOF-Co/AgOTf-4). The same procedure was used as in the synthesis of MOF-Co/$AgBF_4$-1. For a solution containing 1.7 mM [Co(4-papyrdpm)$_3$], 1.7 mM AgOTf, and 1.0 mL of acetonitrile (total volume 4.0 mL) the isolated yield of crystalline material was 6.1 mg (69%). IR (KBr pellet): ν 1607, 1563, 1537, 1411, 1380, 1346, 1282, 1247, 1221, 1160, 1021, 995 cm^{-1}.

[Co(4-papyrdpm)$_3$AgBF$_4$] (MOF-Co/AgBF$_4$-4). The same procedure was used as in the synthesis of MOF-Co/$AgBF_4$-1. For a solution containing 1.7 mM [Co(4-papyrdpm)$_3$], 1.7 mM $AgBF_4$, and 1.0 mL of acetonitrile (total volume 4.0 mL) the isolated yield of crystalline material was 7.5 mg (89%). IR (KBr pellet): ν 1559, 1379, 1346, 1249, 1084, 1042, 1030, 999 cm^{-1}

[Co(4-papyrdpm)$_3$AgPF$_6$] (MOF-Co/AgPF$_6$-4). The same procedure was used as in the synthesis of MOF-Co/$AgBF_4$-1. For a solution containing 1.7 mM [Co(4-papyrdpm)$_3$], 1.7 mM $AgPF_6$, and 1.0 mL of acetonitrile (total volume 4.0 mL) the isolated yield of crystalline material was 6.9 mg (77%). IR (KBr pellet): ν 1159, 1380, 1345, 1249, 1044, 1030, 1000, 843, 816 cm^{-1}.

Anion-Exchange Studies. Crystals of MOF-Co/AgOTf-1 were grown according to the procedure described above for MOF-Co/$AgBF_4$-1.[23] Once single crystals had formed, the mother liquor was removed and quickly replaced with a solution of 30 mM tetrabutylammonium tetrafluoroborate in a 4:1 benzene/acetonitrile mixture. The solution was then gently shaken for 24 h. Single crystals were taken from the solution and analyzed by X-ray diffraction; this net is designated MOF-Co/Ag×BF_4-1, where the "×" designates the exchanged anion. The remaining crystals were washed with a benzene/acetonitrile solution, dried, and analyzed by ^{19}F NMR ($CDCl_3$, 300 MHz, 25 °C) giving signals at −152.1 ppm indicative of the tetrafluoroborate anion. An identical experiment was performed with a 26 mM solution of tetrabutylammonium hexafluorophosphate (MOF-Co/Ag×PF_6-1). ^{19}F NMR ($CDCl_3$ 300 MHz, 25 °C): δ −69.3, −71.8 ppm.

X-ray Crystallographic Analysis. Single crystals of each compound suitable for X-ray diffraction structural determination were mounted on quartz capillaries with Paratone oil and were cooled in a nitrogen stream on the diffractometer. Data were collected on either a Bruker AXS or a Bruker P4 diffractometer each equipped with area detectors. Peak integrations were performed with the Siemens SAINT software package. Absorption corrections were applied using the program SADABS. Space group determinations were performed by the program XPREP. The structures were solved by either Patterson or direct methods and refined with the SHELXTL software package (Sheldrick, G. M. *SHELXTL vers. 5.1 Software Reference Manual*; Bruker AXS: Madison, WI, 1997). All hydrogen atoms were fixed at calculated positions with isotropic thermal parameters, and all non-hydrogen atoms were refined anisotropically unless otherwise noted. Many of the structures contained ordered, disordered, or partially occupied solvent molecules (benzene, acetonitrile); these details are not described in the text below but have been provided in the Supporting Information. Also, several structures had some disorder and/or partial occupancy complications with the anions. Again, the details for each crystallographic analysis can be found in the Supporting Information. Many of the structures refined quite well, those that did not (e.g., R_1 values >10%) are presented solely to demonstrate connectivity and net topology.

Thermogravimetric Analysis. All MOF samples were dried in a vacuum oven at ∼50 °C for 10−12 h prior to analysis. Thermogravimetric analysis (TGA) experiments were run on a TA Instruments Q600 using a platinum pan. Samples of each MOF (∼2−10 mg) were analyzed under a nitrogen flow (100 mL/min) from ∼25 to 1000 °C with a gradient of 20 °C/min.

Results and Discussion

Preparation of Metalloligands. As shown in Chart 1, three metalloligand systems have been prepared and utilized in the MOFs described here. The simplest of these metalloligands, [M(4-pyrdpm)$_3$], has been previously reported, in addition to

Chart 1. List of Ligands, Metalloligands, and General MOF Connectivity.

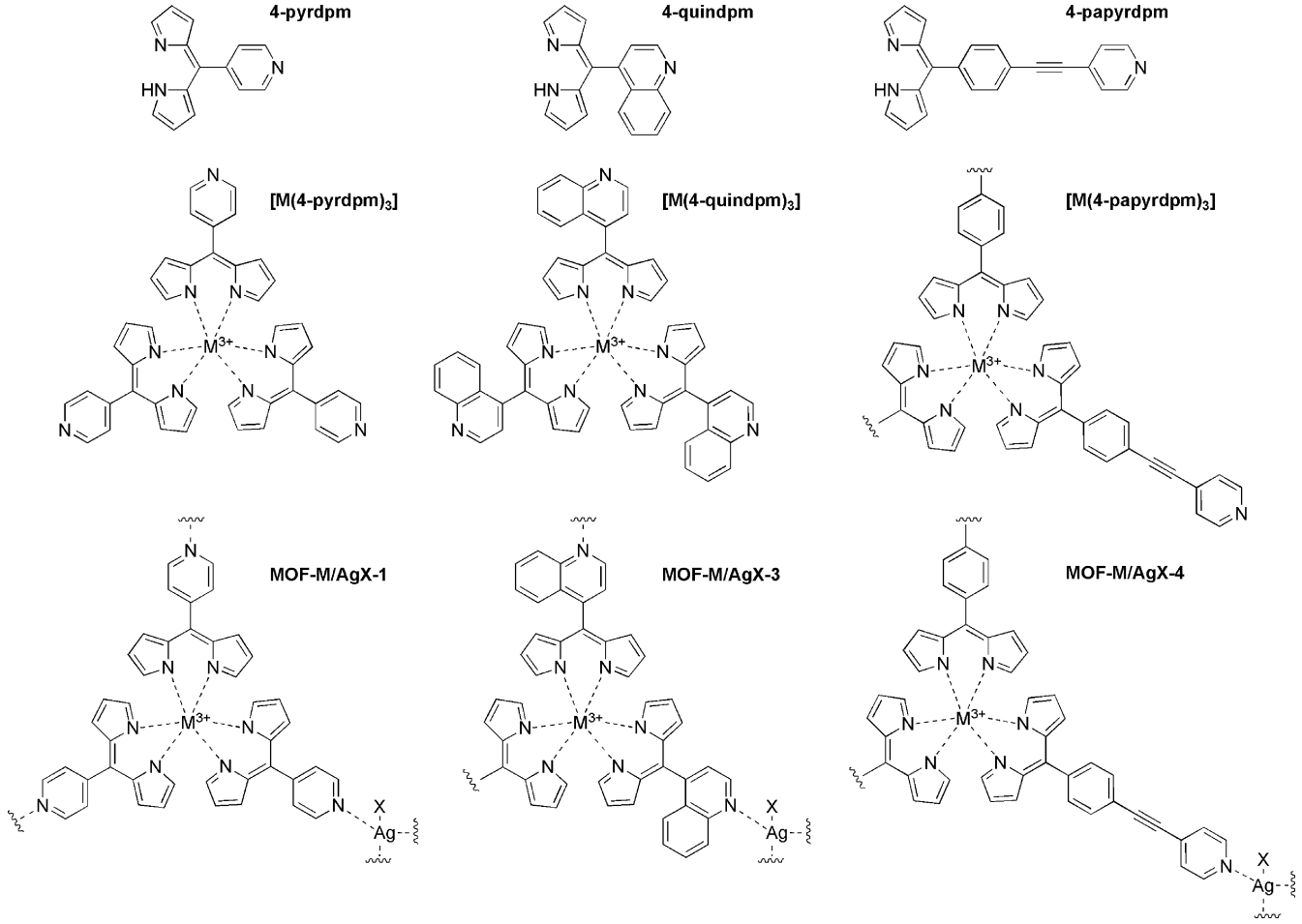

two MOFs prepared from this precursor.[23] The other metalloligands, [M(4-quindpm)$_3$] and [M(4-papyrdpm)$_3$], have not been previously reported, although related molecules have been described in the literature.[29,31] For all three metalloligand systems the synthetic procedure is the same: (1) preparation of the dipyrromethane from condensation of an aryl aldehyde (the precursor aldehyde for 4-papyrdpm was synthesized according to Scheme S1) and pyrrole; (2) oxidation of the dipyrromethane to the dipyrromethene (dipyrrin) using DDQ; and (3) complexation of the dipyrrin to a transition metal salt, either $FeCl_3 \cdot 6H_2O$ or $Na_3[Co(NO_2)_6]$, to generate the desired coordination complex.[23,24,32] The synthesis of these metalloligands proceeds in modest yields; however, the reaction can be scaled to reasonably obtain 500−750 mg quantities of these complexes. Each coordination complex possesses three pendant pyridyl or quinolyl groups, permitting coordination to a second metal ion, and hence can function as a metalloligand. The rich electronic absorption spectra of these metalloligands are characteristic of both the metal ion and the dipyrrinato ligand. All of the dipyrrinato metalloligands display ligand-to-metal charge transfer (LMCT) bands centered at approximately 470 and 510 nm for the cobalt(III) complexes, and 445 and 496 nm for the iron(III) complexes. Additional transitions in the ultraviolet region are attributed to $\pi \rightarrow \pi^*$ transitions of the *meso*-aryl substituents, which are observed at approximately 230 and 290 nm for M(4-pyrdpm)$_3$; 270, 295, and 315 for M(4-quindpm)$_3$; and 228, 279, 293, 335, and 398 nm for Co(4-papyrdpm)$_3$.

Preparation of MOFs: Anion Templating Effects. The synthesis of all MOFs described herein followed previously reported methods.[23] The metalloligand was dissolved in benzene and mixed with one equivalent of a silver(I) salt also dissolved in benzene (combined volume of ∼3 mL); mixing of these two components results in the formation of an orange-red precipitate, which redissolves upon addition of a minimal amount of acetonitrile (≤1 mL). The mixtures were then allowed to evaporate slowly, yielding single crystals in 1−2 weeks. Incorporation of the metalloligand into the extended structure was readily apparent from the deep red or orange color of the crystals (depending on the metal ion), indicative of LMCT bands from the dipyrrin complex.[23,31,32] It is important to note that the synthetic procedure used with these metalloligands is essentially identical to that employed in the synthesis of the analogous organic nitrile MOFs, precluding any need for the development of new synthetic methods.[25−28]

In our previous report, the combination of [Co(4-pyrdpm)$_3$] with AgOTf (OTf$^-$ = triflate, $CF_3SO_3^-$) or [Fe(4-pyrdpm)$_3$] with $AgBF_4$ led to the formation of isostructural, doubly interpenetrated MOF-Co/AgOTf-1 (previously named MOF-Co/Ag-1) and MOF-Fe/$AgBF_4$-1 (previously named MOF-Fe/Ag-1), respectively.[23] Both of these frameworks crystallized in the orthorhombic space group *Pbcn* and possess a (10,3)-d network

(31) Halper, S. R.; Cohen, S. M. *Chem. Eur. J.* **2003**, *9*, 4661−4669.
(32) Cohen, S. M.; Halper, S. R. *Inorg. Chim. Acta* **2002**, *341*, 12−16.

Table 1. X-ray Crystallographic Data for (10,3) Net MOFs Derived from [M(4-pyrdpm)$_3$] (M = Co^{3+}, Fe^{3+})

	MOF-Co/$AgBF_4$-1	MOF-Fe/AgOTf-1	MOF-CoFe/$AgBF_4$-1	MOF-CoFe/AgOTf-1
empirical formula	$C_{84}H_{60}Ag_2B_2Co_2F_8N_{18}$	$C_{160}H_{123}Ag_3F_9Fe_3N_{29}O_9S_3$	$C_{84}H_{60}Ag_2B_2CoF_8FeN_{18}$	$C_{86}H_{60}Ag_2CoF_6FeN_{18}O_6S_2$
crystal system	monoclinic	monoclinic	orthorhombic	orthorhombic
space group	$P2_1/c$	$C2/c$	$Pbcn$	$Pbcn$
unit cell dimensions				
a (Å)	33.41(2)	33.186(5)	26.939(6)	26.813(3)
b (Å)	26.932(16)	66.054(10)	12.335(3)	12.6035(12)
c (Å)	12.365(8)	14.882(2)	33.458(7)	33.472(3)
α (deg)	90	90	90	90
β (deg)	91.533(10)	110.699(2)	90	90
γ (deg)	90	90	90	90
volume (Å^3), z	11123(12), 8	30516(8), 8	11118(4), 4	11311.5(19), 4
crystal size (mm^3)	0.30 × 0.22 × 0.16	0.32 × 0.15 × 0.02	0.38 × 0.34 × 0.30	0.35 × 0.26 × 0.18
temperature (K)	100(2)	100(2)	100(2)	100(2)
reflections collected	94777	133235	99449	96717
independent reflections	24306 [R(int) = 0.0986]	27904[R(int) = 0.1500]	10174 [R(int) = 0.0875]	11551 [R(int) = 0.0431]
data/restraint/parameters	24306/67/1022	27904/0/1953	10174/68/559	11551/0/614
goodness-of-fit on F^2	1.090	1.029	1.030	1.106
Final R indices $I > 2\sigma(I)$[a]	$R1$ = 0.0857	$R1$ = 0.0847	$R1$ = 0.0738	$R1$ = 0.0718
	$wR2$ = 0.2445	$wR2$ = 0.2048	$wR2$ = 0.1880	$wR2$ = 0.1619
R indices (all data)[a]	$R1$ = 0.1155	$R1$ = 0.1620	$R1$ = 0.1256	$R1$ = 0.0796
	$wR2$ = 0.2628	$wR2$ = 0.2314	$wR2$ = 0.2090	$wR2$ = 0.1647

[a] $R1 = \sum||F_o| - |F_c||/\sum|F_o|$, $wR2 = \{\sum[w(F_o^2 - F_c^2)^2]/\sum[wF_o^4]\}^{1/2}$.

topology (Schläfli symbol 10^3, vertex symbol $10_2{\cdot}10_4{\cdot}10_4$),[9] as determined by generation of the vertex symbols using the program OLEX.[33] The (10,3) topology was expected on the basis of comparison to the systems prepared with the organic ligand 1,3,5-tris(4-ethynylbenzonitrile)benzene (TEB) and AgOTf.[25−28]

To demonstrate that the OTf^- and BF_4^- anions result in identical structure types, the complementary frameworks MOF-Co/$AgBF_4$-1 and MOF-Fe/AgOTf-1 were synthesized and characterized. Single crystals of both networks were obtained by slow evaporation, and the MOF structures were determined by X-ray crystallography (Table 1). As shown in Figure 1 and listed in Table 2, MOF-Co/$AgBF_4$-1 and MOF-Fe/AgOTf-1 also form (10,3) networks. As expected, MOF-Co/$AgBF_4$-1 forms a doubly interpenetrated (10,3)-d network;[9] the only difference from the earlier structures is that MOF-Co/$AgBF_4$-1 crystallized in the monoclinic space group $P2_1/c$, (albeit with cell parameters virtually identical to those of earlier reported structures).[23] Of these four structures, MOF-Co/AgOTf-1, MOF-Co/$AgBF_4$-1, MOF-Fe/AgOTf-1, and MOF-Fe/$AgBF_4$-1, only one is not of the (10,3)-d topology (Table 2). Although very similar in overall structure, MOF-Fe/AgOTf-1 was found to form a (10,3)-b framework. The (10,3)-b framework, or $ThSi_2$-type net,[9] has the same Schläfli symbol and vertex symbol descriptors (Schläfli symbol 10^3, vertex symbol $10_2{\cdot}10_4{\cdot}10_4$) as the related (10,3)-d net. Despite the similarities, the (10,3)-b and (10,3)-d nets can be distinguished by comparison to the idealized nets.[9] The differences in the topology of the nets are best realized by inspection of the structures along directions of high symmetry (Figure 1). As found in the other (10,3) nets synthesized here, the structure of MOF-Fe/AgOTf-1 contains two independent, interpenetrated nets. The synthesis and crystallization of MOF-Fe/AgOTf-1 was repeated several times to confirm this surprising finding, and in every case the same (10,3)-b network was obtained. This result led us to examine the role of the counteranions in governing the topology of these MOFs.

To explore the effect of the silver(I) counteranion on the topology of the resultant network, [Co(4-pyrdpm)$_3$] or [Fe(4-pyrdpm)$_3$] was combined with $AgPF_6$ or $AgSbF_6$ to generate four new networks (Table 3): MOF-Co/$AgPF_6$-1, MOF-Co/$AgSbF_6$-1, MOF-Fe/$AgPF_6$-1, and MOF-Fe/$AgSbF_6$-1. In all four MOFs the structure was determined to be a 2D (6,3) honeycomblike network (Schläfli symbol 6,[3] vertex symbol 6·6·6), distinct from the 3D (10,3) nets found with AgOTf and $AgBF_4$ (Table 2). The structures of MOF-Co/$AgPF_6$-1 and MOF-Co/$AgSbF_6$-1 are shown in Figure 2; the isostructural iron(III) analogues are shown in Figure S1. The MOFs consist of 2D nets, with sheets of [M(4-pyrdpm)$_3$] complexes linked by silver(I) ions. Each silver(I) ion is coordinated to three different [M(4-pyrdpm)$_3$] complexes, as found in the (10,3) nets. Each silver(I) ion is also coordinated by an acetonitrile solvent molecule (rather than the PF_6^- or SbF_6^- anion, Figure 3); the coordinated solvent was found in all (6,3) nets, but was not well-ordered in the MOF-M/$AgPF_6$-1 networks (Figure 2). Our findings are consistent with reports that the PF_6^- and SbF_6^- anions can template identical topologies in coordination solids.[34]

The overall (6,3) topology of the MOF-M/$AgPF_6$-1 and MOF-M/$AgSbF_6$-1 frameworks is the same, but the packing of these honeycomb sheets show different layering patterns (Figure S2). In MOF-M/$AgPF_6$-1, the nets lie in the crystallographic *bc*-plane and an *AB* stacking pattern is observed. In MOF-M/$AgSbF_6$-1, the nets lie in the crystallographic *ac*-plane and follow an *ABCD* stacking pattern. Despite the differences between the MOF-M/$AgPF_6$-1 and MOF-M/$AgSbF_6$-1 frameworks, the cobalt(III) and iron(III) nets prepared with the same silver(I) salt are identical (e.g. MOF-Co/$AgPF_6$-1 and MOF-Fe/$AgPF_6$-1 are isostructural). The preservation of structure with either cobalt(III) or iron(III) displays the modular nature of this MOF synthetic approach and indicates that the anions are playing the dominant structure-determining role. Interestingly, in both structure types, each individual layer of the (6,3) net is homochiral, comprising only Δ or Λ tris(chelate) metal centers. Each layer neighbors two enantiomerically pure sheets of opposite chirality (e.g. in MOF-M/$AgSbF_6$-1 if *A* is Δ, then in *ABCD* the chirality of each net alternates as ΔΛΔΛ). The

(33) Dolomanov, O. V.; Blake, A. J.; Champness, N. R.; Schröder, M. *J. Appl. Crystallogr.* **2003**, *36*, 1283−1284.

(34) Dong, Y.-B.; Xu, H.-X.; Ma, J.-P.; Huang, R.-Q. *Inorg. Chem.* **2006**, *45*, 3325−3343.

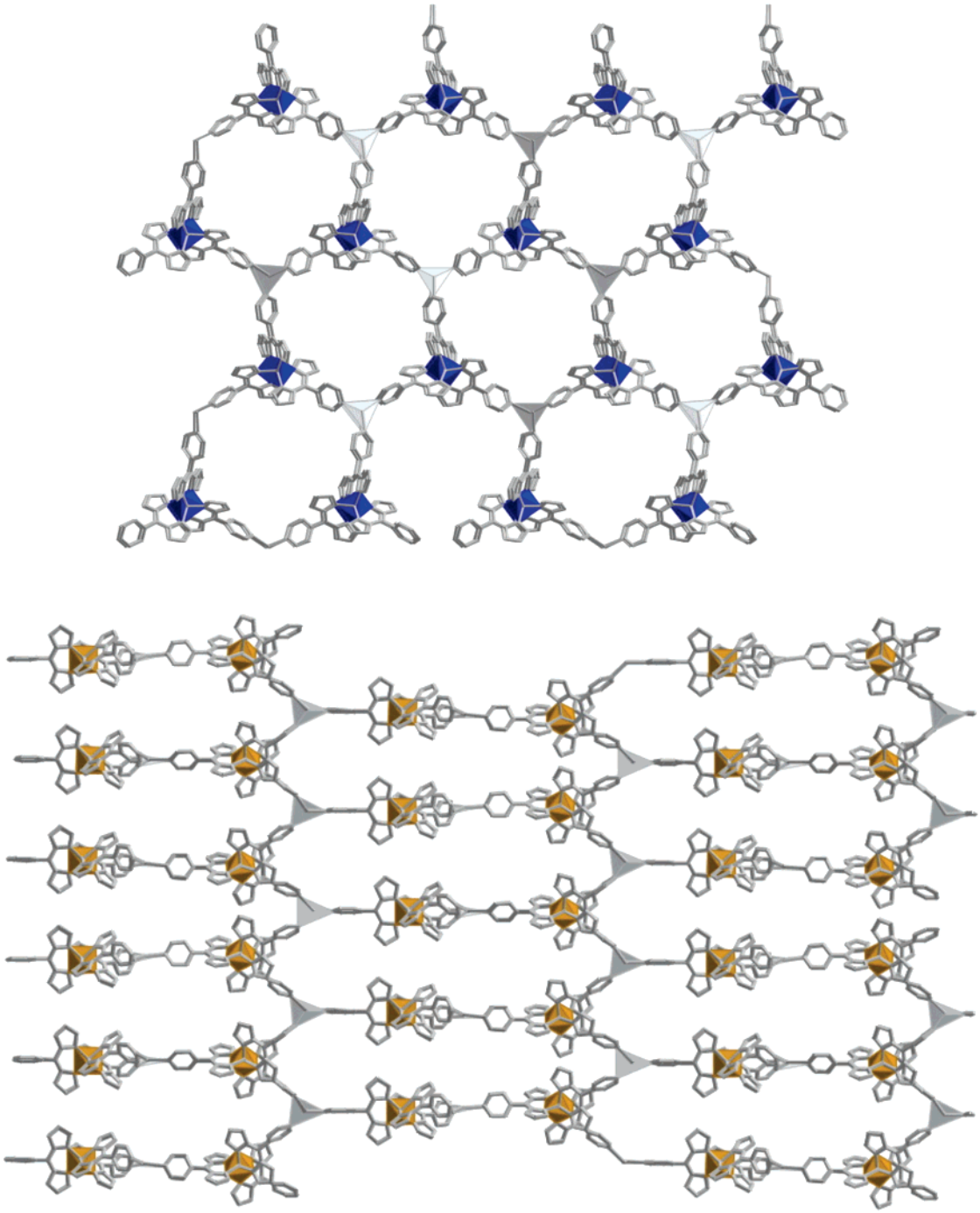

Figure 1. X-ray structure of the 3D (10,3)-d net MOF-Co/$AgBF_4$-1 (top) and the (10,3)-b net MOF-Fe/AgOTf-1 (bottom). The structures are viewed down the crystallographic *c*-axis, showing only one of the two interpenetrated nets for clarity. Cobalt(III), iron(III), and silver(I) centers are represented by blue, gold, and gray polyhedra, respectively. Hydrogen atoms, anions, and solvent molecules have also been omitted for clarity.

homochirality of these 2D sheets is in contrast to those based on three-fold symmetric oxalate metalloligands. In the reported oxalate-based systems both 2- and 3D MOFs are known; the 2D MOFs are racemic, wereas a different set of 3D MOFs were found to be homochiral.[14−16,35] Overall, the anions clearly exhibit a pronounced templating effect in the synthesis of dipyrrinato, metalloligand-derived MOFs. Although never described with the three-fold symmetric 1,3,5-tris(4-ethynylbenzonitrile)benzene ligand, anion templating effects in Ag-nitrile MOFs have been reported in the literature.[36−38]

Noting that the iron(III) and cobalt(III) MOFs are generally isostructural, it was expected that, when using the same silver(I) salt, the synthesis of trimetallic (Fe/Co/Ag) MOFs would be accessible. Under conditions identical to those used for

(35) Pellaux, R.; Schmalle, H. W.; Huber, R.; Fischer, P.; Hauss, T.; Ouladdiaf, B.; Decurtins, S. *Inorg. Chem.* **1997**, *36*, 2301−2308.

(36) Hirsch, K. A.; Venkataraman, D.; Wilson, S. R.; Moore, J. S.; Lee, S. *J. Chem. Soc., Chem. Commun.* **1995**, 2199−2200.

(37) Venkataraman, D.; Lee, S.; Moore, J. S.; Zhang, P.; Hirsch, K. A.; Gardner, G. B.; Covey, A. C.; Prentice, C. L. *Chem. Mater.* **1996**, *8*, 2030−2040.

(38) Hirsch, K. A.; Wilson, S. R.; Moore, J. S. *Inorg. Chem.* **1997**, *36*, 2960−2968.

Table 2. Network Topologies for the MOFs Prepared from Dipyrrin Metalloligands and Silver(I) Salts

framework	M = Co	M = Fe	M = CoFe	interpenetration/stacking
MOF-M/AgOTf-1	(10,3)-d	(10,3)-b	(10,3)-d	two-fold
MOF-M/$AgBF_4$-1	(10,3)-d	(10,3)-d	(10,3)-d	two-fold
MOF-M/$AgPF_6$-1	(6,3)	(6,3)	n.d.	*AB* stacked layers
MOF-M/$AgSbF_6$-1	(6,3)	(6,3)	(6,3)	*ABCD* stacked layers
MOF-M/Ag×BF_4-1	(10,3)-d	n.d.	n.d.	two-fold
MOF-M/Ag×PF_6-1	(10,3)-d	n.d.	n.d.	two-fold
MOF-M/AgOTf-3	n.d.	(10,3)-b	n.d.	two-fold
MOF-M/AgOTf-4	(6,3)	n.d.	n.d.	*AB* stacked layers
MOF-M/$AgBF_4$-4	(6,3)	n.d.	n.d.	*AB* stacked layers
MOF-M/$AgPF_6$-4	(6,3)	n.d.	n.d.	*AB* stacked layers

preparing the aforementioned frameworks, [Fe(4-pyrdpm)$_3$], [Co(4-pyrdpm)$_3$], and $AgBF_4$ were combined to obtain dark-green crystals of MOF-CoFe/$AgBF_4$-1 (Table 1), which was anticipated to be a (10,3)-d net on the basis of the structures of MOF-M/$AgBF_4$-1. X-ray diffraction revealed that MOF-CoFe/$AgBF_4$-1 crystallized in the orthorhombic space group *Pbcn* and is a (10,3)-d net (Table 2) that is isostructural with the parent MOF-M/$AgBF_4$-1 networks (Figure 1).[23] The presence of both iron(III) and cobalt(III) in MOF-CoFe/$AgBF_4$-1 was confirmed by the electronic absorption spectrum of MOF crystals after dissolution in acetonitrile; the resultant solution showed transitions characteristic of both dipyrrin complexes (Figure S7). A second trimetallic MOF was prepared by a combination of [Fe(4-pyrdpm)$_3$], [Co(4-pyrdpm)$_3$], and $AgSbF_6$ in a benzene/acetonitrile solvent mixture. Determination of the cell parameters for MOF-CoFe/$AgSbF_6$-1 was consistent with the (6,3) net cell parameters observed for MOF-Co/$AgSbF_6$-1 and MOF-Fe/$AgSbF_6$-1 (Table 3). Finally, trimetallic MOFs were prepared with [Fe(4-pyrdpm)$_3$], [Co(4-pyrdpm)$_3$], and AgOTf. Single crystals proved more challenging to grow, but were obtained; X-ray diffraction revealed a doubly interpenetrated (10,3)-d net crystallized in the orthorhombic space group *Pbcn* (Table 1). The space group, cell parameters, and topology are identical to those of one of the parent networks, MOF-Co/AgOTf-1.[23] The (10,3)-d net is the same topology found for MOF-Co/AgOTf-1, MOF-M/$AgBF_4$-1, MOF-CoFe/$AgBF_4$-1, but not for MOF-Fe/AgOTf-1 (which formed the slightly different (10,3)-b net). In this case, where the iron(III) and cobalt(III) monomers form slightly different MOF topologies, the more commonly observed (10,3)-d net predominates. Overall, these results show that multimetallic MOFs can be prepared and that the MOF structure can be predicted on the basis of individual metalloligand systems.

Silver(I) Coordination Environments. For the (10,3)-d networks (MOF-Co/AgOTf-1, MOF-Co/$AgBF_4$-1, MOF-Fe/$AgBF_4$-1, MOF-CoFe/AgOTf-1, MOF-CoFe/$AgBF_4$-1), the silver(I) ions generally adopt a distorted trigonal pyramidal arrangement (Figure 3), in which the metal center is occupied by three pyridyl nitrogen atoms (from three different metalloligands) and by either an oxygen or fluorine atom from the weakly coordinated anion in the apical position (Table S2). The Ag−N distances lie in the range of 2.21−2.28 Å (sum of van der Waals radii 3.27 Å)[39] and the three Ag−N bonds form a nonideal trigonal plane, with N−Ag−N angles of ∼110−125°. The interaction between the silver(I) ion and the fourth ligating atom (from the anion) exhibit slightly different Ag−X (X = O, F) distances and N−Ag−X angles in each structure. Binding of the OTf^- anion to silver(I) was found to have a Ag−O distance of ∼2.57 Å (sum of van der Waals radii 3.24 Å)[39] for both MOF-Co/AgOTf-1 and MOF-CoFe/AgOTf-1. Similar bond lengths and angles were observed in the MOF-M/$AgBF_4$-1 structures (Table S2). The Ag−F contacts in MOF-Fe/$AgBF_4$-1 and MOF-CoFe/$AgBF_4$-1 were found to be 2.69 and 2.60 Å, respectively (sum of van der Waals radii 3.19 Å).[39] MOF-Co/$AgBF_4$-1 actually has two independent silver(I) centers, with similar Ag−F contacts of 2.52 and 2.58 Å. While the anions (OTf^- and BF_4^-) are located within the cavity of two interpenetrated (10,3)-d nets, they are coordinated to only one silver(I) center, even though the position of the anions is suggestive of a bridging interaction between the two adjacent networks.

While structurally similar to the (10,3)-d nets, the (10,3)-b net MOF-Fe/AgOTf-1 possesses four distinct silver(I) coordination environments. At two of the silver(I) centers there are no close contacts to the anions (<3.0 Å), generating a trigonal planar center (although there are OTf^- anions in proximity to

Table 3. X-ray Crystallographic Data for (6,3) Net MOFs Derived from [M(4-pyrdpm)$_3$] (M = Co^{3+}, Fe^{3+})

	MOF-Co/$AgPF_6$-1	MOF-Fe/$AgPF_6$-1	MOF-Co/$AgSbF_6$-1	MOF-Fe/$AgSbF_6$-1
empirical formula	$C_{45}H_{33}AgCoF_6N_9P$	$C_{58}H_{43.5}AgF_6FeN_{12.5}P$	$C_{54.2}H_{43.2}AgCoF_6N_{10}Sb$	$C_{53}H_{42}AgF_6FeN_{10}Sb$
crystal system	triclinic	triclinic	monoclinic	monoclinic
space group	$P\bar{1}$	$P\bar{1}$	$P2_1/c$	$P2_1/c$
unit cell dimensions				
a (Å)	13.120(3)	13.089(3)	15.7911(14)	15.874(2)
b (Å)	16.111(3)	16.265(3)	25.454(2)	24.606(3)
c (Å)	16.134(3)	16.105(3)	16.3779(14)	16.377(2)
α (deg)	110.178(3)	110.124(3)	90	90
β (deg)	112.416(3)	112.084(3)	109.8240(10)	110.009(2)
γ (deg)	97.335(3)	98.571(3)	90	90
volume (Å^3), z	2824.0(10), 2	2826.3(9), 2	6193.0(9), 4	6010.7(13), 4
crystal size (mm^3)	0.50 × 0.30 × 0.23	0.47 × 0.41 × 0.18	0.53 × 0.50 × 0.45	0.22 × 0.20 × 0.04
temperature (K)	100(2)	100(2)	100(2)	100(2)
reflections collected	23611	23676	49135	44457
independent reflections	10212 [R(int) = 0.0353]	10208 [R(int) = 0.0295]	12651 [R(int) = 0.0386]	10996 [R(int) = 0.0622]
data/restraint/parameters	10212/0/616	10208/63/899	12651/17/757	10996/17/683
goodness-of-fit on F^2	1.072	1.053	1.042	1.078
final R indices I > 2σ(I)[a]	$R1$ = 0.0652	$R1$ = 0.0508	$R1$ = 0.0695	$R1$ = 0.1070
	$wR2$ = 0.1765	$wR2$ = 0.1347	$wR2$ = 0.1902	$wR2$ = 0.2651
R indices (all data)[a]	$R1$ = 0.0739	$R1$ = 0.0683	$R1$ = 0.0802	$R1$ = 0.1297
	$wR2$ = 0.1815	$wR2$ = 0.1449	$wR2$ = 0.1968	$wR2$ = 0.2759

[a] $R1 = \sum||F_o| - |F_c||/\sum|F_o|$, $wR2 = \{\sum[w(F_o^2 - F_c^2)^2]/\sum[wF_o^4]\}^{1/2}$.

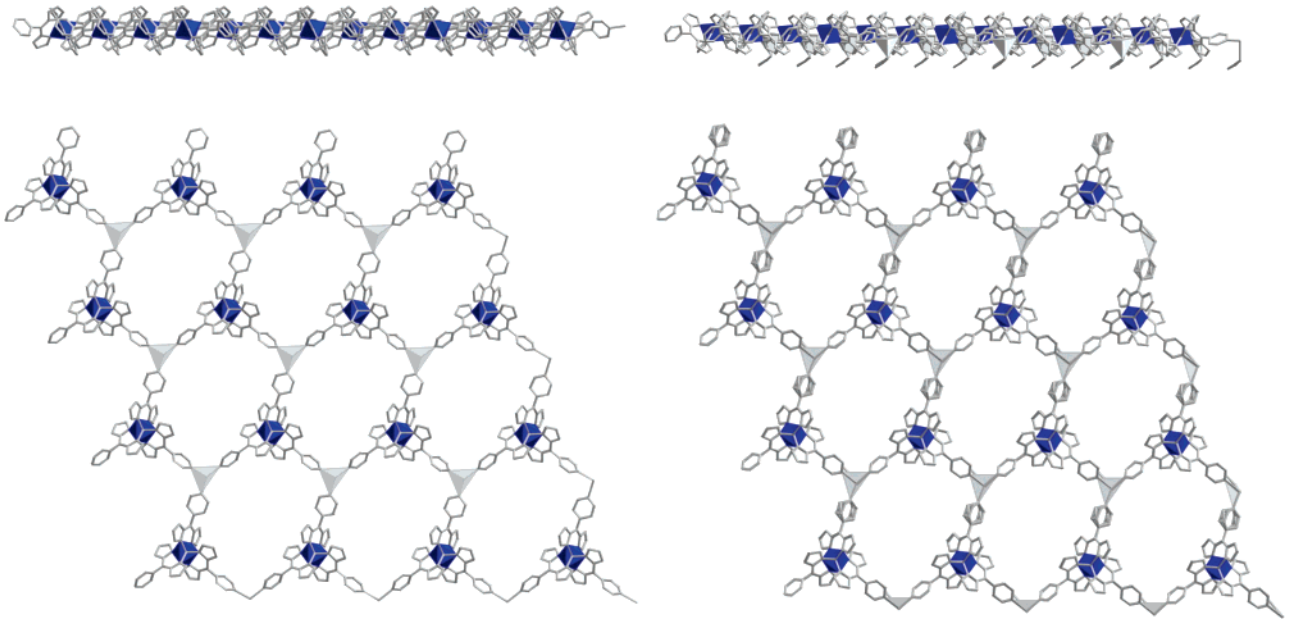

Figure 2. X-ray structure of (6,3) nets MOF-Co/$AgPF_6$-1 (left) and MOF-Co/$AgSbF_6$-1 (right). Cobalt(III) and silver(I) centers are represented by blue and gray polyhedra, respectively. The top view of these MOFs is along the plane of the (6,3) net; for MOF-Co/$AgPF_6$-1 this is the crystallographic *bc*-plane and for MOF-Co/$AgSbF_6$-1 this is the crystallographic *ac*-plane. The bottom views are roughly 90° normal to these planes (90° rotation relative to the top perspectives). Hydrogen atoms and anions have been omitted for clarity. All solvent molecules, except for the apical, silver(I)-coordinated acetonitrile molecules in MOF-Co/$AgSbF_6$-1, have been omitted for clarity. The corresponding MOF-Fe/AgX-1 compounds are isostructural (see Supporting Information).

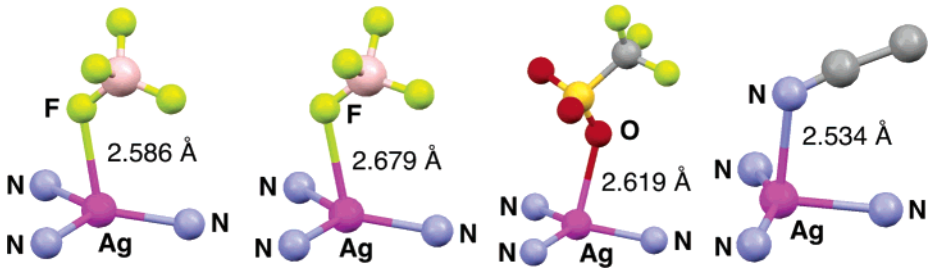

Figure 3. Representative coordination environments at the silver(I) ions in (from left to right): MOF-Co/$AgBF_4$-1, MOF-Co/Ag×BF_4-1, MOF-Fe/AgOTf-1, and MOF-Co/$AgSbF_6$-1. Only the coordinating anions or solvent and pyridyl nitrogen atoms are shown for clarity. Bond length shown is between the silver(I) ion and coordinating anion/solvent molecule. Colors: boron (pale pink), carbon (gray), nitrogen (blue), oxygen (red), fluorine (yellow), sulfur (orange), and silver (magenta).

the silver(I) ions in the lattice). At the third silver(I) center there is a close contact to one OTf^- anion at 2.62 Å for a trigonal pyramidal geometry (Figure 3). Finally, the fourth silver(I) ion in MOF-Fe/AgOTf-1 has two close contacts with OTf^- anions, with Ag−O bond lengths of 2.66 and 2.71 Å. The two oxygen atoms in this third silver(I) center are bound axially to the resultant trigonal bipyramidal silver(I) center.

Similar to the (10,3) nets, the metalloligands in the (6,3) MOFs are assembled by a three-fold linkage of the peripheral nitrogen atoms of the metalloligand to the silver(I) center with Ag−N bonds lengths of 2.20−2.38 Å. In contrast to the (10,3) nets, the trigonal plane of the silver(I) centers in the (6,3) nets undergo a significant distortion toward T-shape (Figure 3), with one N−Ag−N angle substantially more obtuse (145−150°) than the other two (Table S3). Unlike the 3D MOFs described, the apical position of the silver(I) centers are not bound by anions. The anions in these structures are intercalated between the graphitelike sheets of the MOF, exhibiting no close interactions between the anions and the silver(I) ions. Rather, in all four MOF-M/$AgPF_6$-1 and MOF-M/$AgSbF_6$-1 networks the apical position of silver(I) ion is bound by the nitrogen atom of an acetonitrile solvent molecule, to give an overall trigonal pyramidal coordination sphere (Figure 3). In the MOF-M/$AgSbF_6$-1 networks the solvent was reasonably well ordered with Ag−N (CH_3CN) distances of 2.50−2.53 Å, within the sum of the van der Waals radii (3.27 Å).[39]

Anion-Exchange Reactions. Having observed a pronounced anion templating effect in the series of MOF-M/AgX-1 structures, we sought to elucidate the origin of this anion effect and to determine whether any of these MOFs were stable to anion-exchange conditions. To probe this effect, single crystals of MOF-Co/AgOTf-1 were grown as described,[23] followed by removal of the mother liquor and rapid replacement with a 4:1 benzene/acetonitrile solution containing 30 mM tetrabutylammonium tetrafluoroborate. The solution was then gently shaken for ~24 h. No significant dissolution or change in morphology of the original MOF-Co/AgOTf-1 crystals was observed in this time period; single crystals were removed from the tetrabutylammonium tetrafluoroborate solution and analyzed by X-ray diffraction (Table 4). The resultant framework (MOF-Co/Ag×BF_4-1, the × designates an exchanged anion) is identical to the parent structure (Figure 4); complete anion exchange is

(39) Bondi, A. *J. Phys. Chem.* **1964**, *68*, 441−451.

Table 4. X-ray Crystallographic Data for Anion-Exchange Experiments on (10,3) Net MOF-Co/AgOTf-1

	MOF-Co/AgOTf-1[b]	MOF-Co/Ag×BF_4-1	MOF-Co/Ag×PF_6-1
empirical formula	$C_{55}H_{48}AgCoF_3N_{15}O_3S$	$C_{42}H_{30}AgBCoF_4N_9$	$C_{42}H_{30}AgCoF_6N_9P$
crystal system	orthorhombic	orthorhombic	orthorhombic
space group	*Pbcn*	*Pbcn*	*Pbcn*
unit cell dimensions			
a (Å)	26.713(3)	26.914(7)	26.847(2)
b (Å)	12.5800(13)	12.327(3)	12.6272(10)
c (Å)	33.455(3)	33.375(8)	33.438(3)
α (deg)	90	90	90
β (deg)	90	90	90
γ (deg)	90	90	90
volume (Å^3), *z*	11243(2), 8	11073(5), 8	11335.5(15), 8
crystal size (mm^3)	0.40 × 0.33 × 0.15	0.30 × 0.20 × 0.10	0.55 × 0.34 × 0.22
temperature (K)	100(2)	100(2)	100(2)
reflections collected	93010	97394	96034
independent reflections	12681 [*R*(int) = 0.0828]	10133 [*R*(int) = 0.1194]	12951 [*R*(int) = 0.0558]
data/restraint/parameters	12681/0/574	10133/16/551	12951/0/578
goodness-of-fit on F^2	1.041	1.045	1.062
final *R* indices $I > 2\sigma(I)$[a]	$R1 = 0.0704$	$R1 = 0.0975$	$R1 = 0.0514$
	$wR2 = 0.1842$	$wR2 = 0.2579$	$wR2 = 0.1316$
R indices (all data) *a*	$R1 = 0.0921$	$R1 = 0.1575$	$R1 = 0.0756$
	$wR2 = 0.1946$	$wR2 = 0.2856$	$wR2 = 0.1396$

[a] $R1 = \sum||F_o| - |F_c||/\sum|F_o|$, $wR2 = \{\sum[w(F_o^2 - F_c^2)^2]/\sum[wF_o^4]\}^{1/2}$. [b] Taken from ref 23.

observed with preservation of the (10,3)-d network topology that is common to both MOF-Co/AgOTf-1 and MOF-Co/$AgBF_4$-1. The tetrafluoroborate anions occupy the same positions in the crystal lattice as the displaced triflate anions (Figure 4) at a similar distance and geometry as found in MOF-Co/$AgBF_4$-1 (Figure 3). Taking crystals of MOF-Co/Ag×BF_4-1, rinsing them with a 4:1 benzene/acetonitrile solution, and dissolving the dried crystals in either $CDCl_3$ or d_6-DMSO and examining the ^{19}F NMR confirmed the complete exchange of anions; a single resonance at −152.1 ppm was the only spectral feature observed, consistent with the tetrafluoroborate anion.

An identical experiment was performed using MOF-Co/AgOTf-1 and tetrabutylammonium hexafluorophosphate. In this case, MOF-Co/AgOTf-1 is a (10,3)-d net while MOF-Co/$AgPF_6$-1 is a (6,3) net; therefore, it was unclear whether anion exchange would occur, if the framework would be stable, and what the structure of the resulting MOF would be. As in the earlier experiment, no change in crystal morphology or stability was observed during the anion-exchange process. After ∼24 h exposure to tetrabutylammonium hexafluorophosphate, single crystals were analyzed to reveal the structure of MOF-Co/Ag×PF_6-1. MOF-Co/Ag×PF_6-1 retains the (10,3)-d net topology while achieving complete anion exchange of the triflate counterions. As in the previous example, the PF_6^- anions occupy the same positions in the crystal lattice as the displaced triflate anions (Figure 4). ^{19}F NMR again confirmed the complete exchange of the triflate anions for PF_6^-, with resonances at −69.3 and −71.8 ppm (a doublet is observed due to coupling to the ^{31}P nucleus). The ability of the large PF_6^- anion to completely displace the triflate anion in MOF-Co/AgOTf-1 strongly suggests that the templating effect observed in these MOFs is not due exclusively to anion size. Clearly, the PF_6^- can fit within the (10,3)-d net with minimal structural perturbations, and therefore it must be some other property of the anion that leads to the formation of a (6,3) net during MOF synthesis in the presence of either PF_6^- or SbF_6^-. Anion-exchange experiments with some of the (6,3) nets described here resulted in loss of crystallinity, and were not pursued further. These findings suggest that in MOF-Co/AgOTf-1 the anion may be important in templating the formation of the MOF, but a specific anion is not required for maintaining the structural stability of the resulting framework.

The aforementioned anion-exchange experiments are notable for several reasons. One important observation is that both experiments described represent an apparent single-crystal-to-single-crystal transformation, where the MOF was sufficiently robust to characterize by high-resolution X-ray diffraction. We are unaware of anion-exchange reactions confirmed by single-crystal X-ray diffraction in MOFs; the use of powder diffraction is common[40−44] and solid-state NMR has also been used,[45] but to our knowledge, single crystal analysis after anion exchange is unprecedented (although examples of single-crystal-to-single-crystal solvent exchange are known).[46−48] Although the preservation of the MOF topology as confirmed by X-ray diffraction is compelling evidence for the proposed single-crystal-to-single-crystal transformation, it should be noted that we cannot entirely rule out the role of a dissolution process in the anion exchange.[49] To absolutely confirm a single-crystal-to-single-crystal transformation, rigorous microscopy studies must be performed. Nevertheless, the ability to perform these experiments and characterize the MOFs in this manner suggests that MOF-Co/AgOTf-1 is quite robust.

Another important observation is that both experiments demonstrate anion exchange against the generally reported trends for anion coordinative ability. Several studies, most recently by Jung et al.,[41,50] have reported on numerous anion-exchange

(40) Hamilton, B. H.; Kelly, K. A.; Wagler, T. A.; Espe, M. P.; Ziegler, C. J. *Inorg. Chem.* **2002**, *41*, 4984−4986.
(41) Jung, O.-S.; Kim, Y. J.; Lee, Y.-A.; Park, K.-M.; Lee, S. S. *Inorg. Chem.* **2003**, *42*, 844−850.
(42) Min, K. S.; Suh, M. P. *J. Am. Chem. Soc.* **2000**, *122*, 6834−6840.
(43) Zhao, W.; Fan, J.; Okamura, T.-a.; Sun, W.-Y.; Ueyama, N. *New J. Chem.* **2004**, *28*, 1142−11550.
(44) Zhao, W.; Fan, J.; Okamura, T.-a.; Sun, W.-Y.; Ueyama, N. *Microporous Mesoporous Mater.* **2005**, *78*, 265−279.
(45) Hamilton, B. H.; Wagler, T. A.; Espe, M. P.; Ziegler, C. J. *Inorg. Chem.* **2005**, *44*, 4891−4893.
(46) Wu, C.-D.; Lin, W. B. *Angew. Chem., Int. Ed.* **2005**, *44*, 1958−1961.
(47) Choi, H. J.; Suh, M. P. *J. Am. Chem. Soc.* **2004**, *126*, 15844−15851.
(48) Deiters, E.; Bulach, V.; Hosseini, M. W. *Chem. Commun.* **2005**, 3906−3908.
(49) Thompson, C.; Champness, N. R.; Khlobystov, A. N.; Roberts, C. J.; Schroder, M.; Tendler, S. J. B.; Wilkinson, M. J. *J. Microsc. (Oxford)* **2004**, *214*, 261−271.
(50) Lee, J. W.; Kim, E. A.; Kim, Y. J.; Lee, Y.-A.; Pak, Y.; Jung, O.-S. *Inorg. Chem.* **2005**, *44*, 3151−3155.

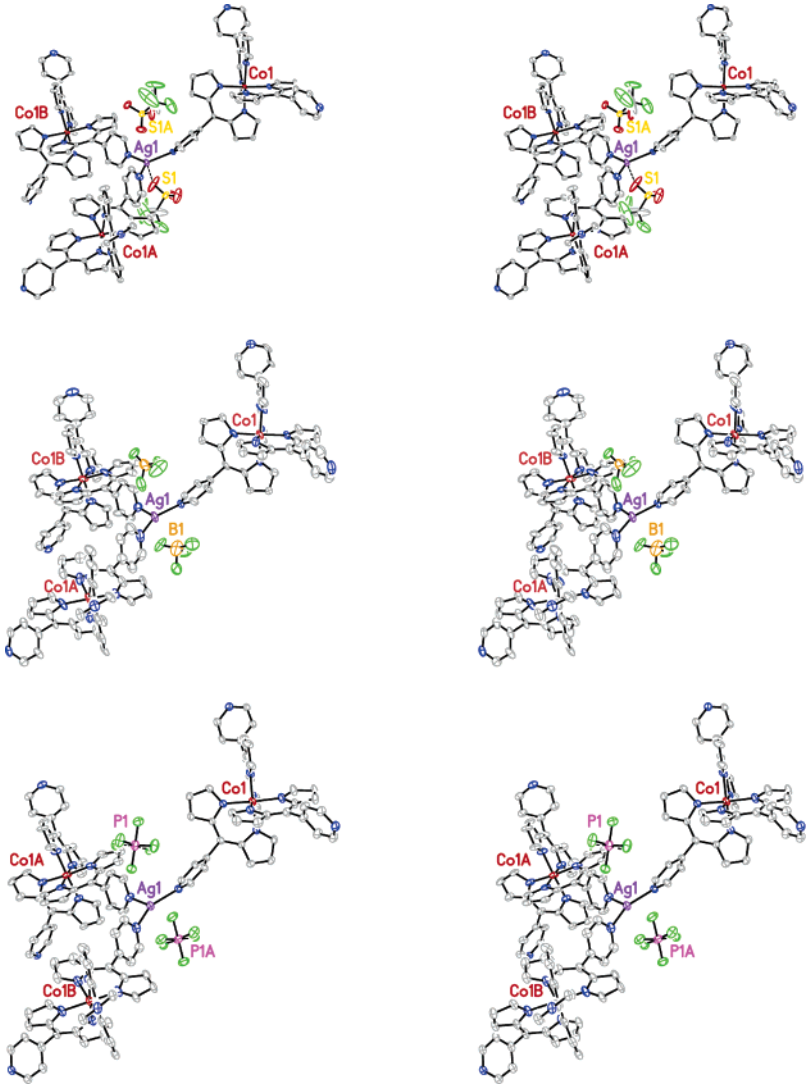

Figure 4. Stereoview of MOF-Co/AgOTf-1 highlighting the location of the anions before (top) and after anion exchange with either tetrabutylammonium tetrafluoroborate (MOF-Co/Ag×BF_4-1, middle) or tetrabutylammonium hexafluorophosphate (MOF-Co/Ag×PF_6-1, bottom). The structure is depicted using 30% thermal ellipsoids. Solvent molecules have been omitted for clarity.

experiments in coordination solids and used their observations to establish a trend from strongly to weakly coordinating anions: NO_2^- > NO_3^- > $CF_3CO_2^-$ > $CF_3SO_3^-$ > PF_6^- > ClO_4^- > BF_4^-.[41] The X-ray structure determinations and ^{19}F NMR experiments performed here show the ability of PF_6^- and BF_4^- to displace the $CF_3SO_3^-$ (OTf^-) anion from MOF-Co/AgOTf-1. Furthermore, on the basis of the aforementioned series, the strongest coordinating anion (OTf^-) and weakest coordinating anion (BF_4^-) examined both generate (10,3) nets. Therefore, we conclude that the coordinative ability of the anion does not play a significant role in the templating effect observed in these MOFs.

MOFs with Modified Dipyrrin Metalloligands. Two additional metalloligand systems were explored in order to determine how changes in metalloligand structure would affect the anion templating effect and hence the topology of the resultant MOFs. The first of these systems were quinoline derivatives of the previously prepared systems, namely [M(4-quindpm)$_3$]. The structure of both metalloligands, [Co(4-quindpm)$_3$] and [Fe(4-quindpm)$_3$], were determined (Table 5); the structures are unremarkable and generally consistent with the related [M(4-pyrdpm)$_3$] complexes (Figure S4, Figure 5).[23] MOFs were prepared under the same conditions used with [M(4-pyrdpm)$_3$], and crystalline materials were readily obtained. In general, the quality and stability of these MOF crystals, designated MOF-M/AgX-3, were poorer than those obtained for MOF-M/AgX-1. Although structural characterization proved more challenging, the structure of MOF-Fe/AgOTf-3 was determined. As shown in Figure 5, the structure of MOF-Fe/AgOTf-3 reveals a (10,3)-b net in the orthorhombic space group *Fddd*. Although the space group and cell parameters differ, MOF-Fe/AgOTf-3 forms the same doubly interpenetrated (10,3)-b network topology ($ThSi_2$-type net, Schläfli symbol 10^3, vertex symbol $10_2{\cdot}10_4{\cdot}10_4$) as MOF-Fe/AgOTf-1. The framework structure is well ordered, with the exception of one of the quinoline rings, which is disordered with respect to a glide plan (see Supporting Information). Also, the location of the OTf^- anions in this structure could not be reliably determined (see Supporting Information); thus, no comments can be provided on their location in the structure in comparison to the other MOFs described here. Although the structure of MOF-Fe/AgOTf-3 is not of high quality, it is sufficient to show the

Table 5. X-ray Crystallographic Data for Metalloligands [M(4-quindpm)$_3$] (M = Co^{3+}, Fe^{3+}) and the Resultant Framework MOF-Fe/AgOTf-3

	[Co(4-quindpm)$_3$]	[Fe(4-quindpm)$_3$]	MOF-Fe/AgOTf-3
empirical formula	$C_{54}H_{36}CoN_3$	$C_{54}H_{36}FeN_9$	$C_{54}H_{36}AgFeN_9$
crystal system	rhombohedral	rhombohedral	orthorhombic
space group	$R\bar{3}$	$R\bar{3}$	*Fddd*
unit cell dimensions			
a (Å)	25.322(5)	25.335(8)	24.601(5)
b (Å)	25.322(5)	25.335(8)	16.546(4)
c (Å)	14.746(6)	14.613(9)	65.775(14)
α (deg)	90	90	90
β (deg)	90	90	90
γ (deg)	120	120	90
volume (Å^3), *z*	8188(4), 6	8123(6), 6	26773(10), 16
crystal size (mm^3)	0.32 × 0.22 × 0.12	0.55 × 0.54 × 0.08	0.28 × 0.21 × 0.13
temperature (K)	100(2)	100(2)	150(2)
reflections collected	22921	23026	57467
independent reflections	3728 [*R*(int) = 0.0601]	3697 [*R*(int) = 0.0371]	6142 [*R*(int) = 0.1179]
data/restraint/parameters	3728/ 0/193	3697/0/193	6142/3/260
goodness-of-fit on F^2	1.116	1.136	0.756
final *R* indices $I > 2\sigma(I)$[a]	*R*1 = 0.0732	*R*1 = 0.0759	*R*1 = 0.0608
	*wR*2 = 0.2469	*wR*2 = 0.2468	*wR*2 = 0.1638
R indices (all data)[a]	*R*1 = 0.0941	*R*1 = 0.0872	*R*1 = 0.1132
	*wR*2 = 0.2615	*wR*2 = 0.2563	*wR*2 = 0.1809

[a] $R1 = \sum||F_o| - |F_c||/\sum|F_o|$, $wR2 = \{\sum[w(F_o^2 - F_c^2)^2]/\sum[wF_o^4]\}^{1/2}$.

network connectivity. Overall, this finding suggests that modification of the metalloligand from a pyridyl to a quinolyl-derivatized dipyrrin does not substantially change the overall MOF topology and that the templating effect of the anion is preserved.

The second modification made to the basic metalloligand system utilized here was an extension of the metalloligand framework by insertion of a rigid phenylethynyl spacer between the dipyrrin and pyridyl binding groups in [M(4-papyrdpm)$_3$]. The structure of [Co(4-papyrdpm)$_3$] was determined (Table 6) and shows the expected geometry (Figure 6). Like other dipyrrinato complexes with elongated meso substitutents,[31] the pendant arms surrounding [Co(4-papyrdpm)$_3$] are slightly bent. Combination of [Co(4-papyrdpm)$_3$] with AgOTf, $AgBF_4$, or $AgPF_6$ under standard crystallization conditions generated single crystals suitable for X-ray analysis. Interestingly, the structures of MOF-Co/AgOTf-4, MOF-Co/$AgBF_4$-4, and MOF-Co/$AgPF_6$-4 (Figure 6) revealed the formation of extended (6,3) nets (Schläfli symbol 6^3, vertex symbol 6•6•6). The three MOFs are essentially isostructural (Table 6). All three of the 2D nets MOF-Co/AgX-4 show a tightly packed, head-to-tail *AB* stacking pattern, with the anions located in an interdigitated fashion near, but not coordinated to, the silver(I) centers. The planes of these honeycomblike sheets are not oriented coincident with any of the crystallographic axes. As in the other (6,3) nets described, each individual layer is homochiral, comprising only Δ or Λ tris(chelate) metal centers (alternating ΔΛ with the *AB* stacking pattern). Also similar to the other (6,3) nets, the silver(I) coordination sphere shows a distortion toward T-shape in the trigonal plane, with one larger N−Ag−N angle of ∼140° (Table S3). Among these three MOFs, only MOF-Co/AgOTf-4 shows a significant bonding interaction between the silver(I) ion and the anion, with a Ag−O distance of 2.60 Å, similar to the Ag−O distances found in MOF-Co/AgOTf-1 and MOF-CoFe/AgOTf-1. For MOF-Co/$AgBF_4$-4 and MOF-Co/$AgPF_6$-4 the anions are not coordinated with distant Ag−F contacts of 2.86 and 2.81 Å, respectively.

The structures of MOF-Co/AgOTf-4 and MOF-Co/$AgBF_4$-4 are a striking contrast to the structures of MOF-Co/AgOTf-1 and MOF-Co/$AgBF_4$-1 which both form (10,3)-d network topologies.[23] This finding shows that some modifications of the ligand system can override the anion templating effect. Changes

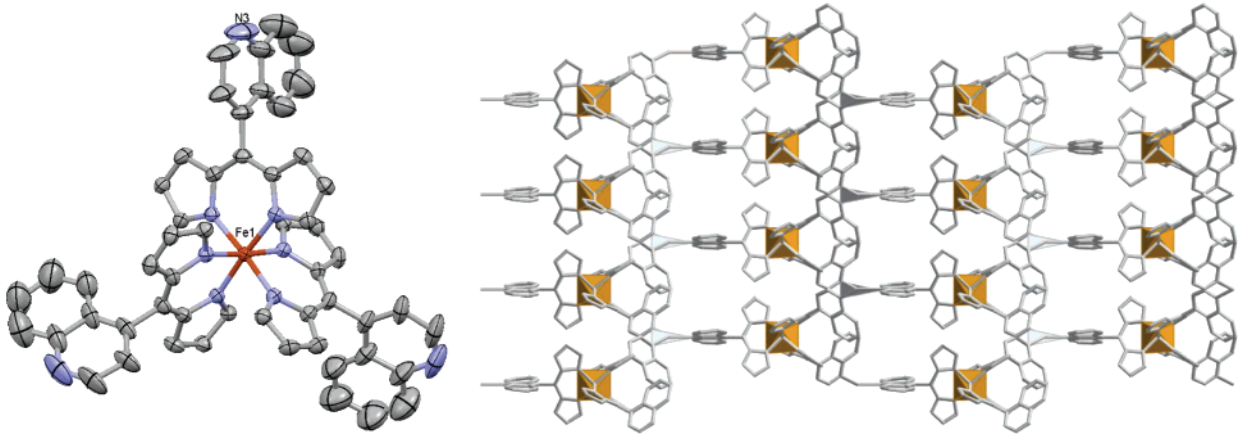

Figure 5. Structural diagram of [Fe(4-quindpm)$_3$] (left) with partial atom numbering scheme (ORTEP, 50% probability ellipsoids). X-ray structure of the (10,3) net MOF-Fe/AgOTf-3 (right) viewed down the crystallographic *a*-axis (only one of two interpenetrated nets are shown, disorder in the quinoline fragment of one dipyrrinato ligand shown). Iron(III) and silver(I) centers are represented by gold and gray polyhedra, respectively. Hydrogen atoms, anions, and solvent molecules have been omitted for clarity.

Table 6. X-ray Crystallographic Data for Metalloligands [Co(4-papyrdpm)$_3$] and the Resultant Frameworks MOF-Co/AgX-4 (X = OTf^-, BF_4^-, PF_6^-)

	[Co(4-papyrdpm)$_3$]	MOF-Co/AgOTf-4	MOF-Co/AgBF$_4$-4	MOF-Co/AgPF$_6$-4
empirical formula	$C_{145}H_{113}Cl_3Co_2N_{18}$	$C_{93}H_{69}AgCoF_3N_{10}O_3S$	$C_{74}H_{51}AgBCoF_4N_{10}$	$C_{90}H_{66}AgCoF_6N_9P$
crystal system	triclinic	triclinic	triclinic	triclinic
space group	$P\bar{1}$	$P\bar{1}$	$P\bar{1}$	$P\bar{1}$
unit cell dimensions				
a (Å)	15.2681(12)	9.3693(9)	9.4031(17)	9.4026(13)
b (Å)	20.2619(16)	19.3886(19)	18.794(4)	19.385(3)
c (Å)	21.5668(17)	22.869(2)	22.803(4)	22.645(3)
α (deg)	69.4900(10)	94.659(2)	91.311(3)	93.820(2)
β (deg)	84.2850(10)	94.855(2)	94.990(3)	95.353(2)
γ (deg)	87.069(2)	91.655(2)	94.994(3)	92.800(2)
volume (Å^3), z	6217.0(8), 2	4123.0(7), 2	3997.5(13), 2	4094.0(10), 2
crystal size (mm^3)	0.27 × 0.26 × 0.10	0.90 × 0.24 × 0.20	0.50 × 0.15 × 0.09	0.44 × 0.17 × 0.07
temperature (K)	100(2)	100(2)	100(2)	100(2)
reflections collected	53738	35002	33394	33968
independent reflections	22587 [R(int) = 0.0440]	14945 [R(int) = 0.0261]	14466 [R(int) = 0.0415]	14809 [R(int) = 0.0548]
data/restraint/parameters	22587/0/1479	14945/0/982	14466/0/876	14809/0/973
goodness-of-fit on F^2	1.063	1.045	0.944	1.043
final R indices $I > 2\sigma(I)$[a]	$R1$ = 0.0661	$R1$ = 0.0468	$R1$ = 0.0663	$R1$ = 0.0845
	$wR2$ = 0.1666	$wR2$ = 0.1188	$wR2$ = 0.1713	$wR2$ = 0.2210
R indices (all data)[a]	$R1$ = 0.0989	$R1$ = 0.0569	$R1$ = 0.0843	$R1$ = 0.1213
	$wR2$ = 0.1810	$wR2$ = 0.1230	$wR2$ = 0.1790	$wR2$ = 0.235

[a] $R1 = \sum||F_o| - |F_c||/\sum|F_o|$, $wR2 = \{\sum[w(F_o^2 - F_c^2)^2]/\sum[wF_o^4]\}^{1/2}$.

in MOF topology due to lengthening of the metalloligand in [Co(4-papyrdpm)$_3$] directly parallels findings from the organic MOF literature. Networks synthesized by Lee and co-workers with 1,3,5-tris(4-ethylbenzonitrile)benzene (TEB) and AgOTf form a (10,3)-b network structure, but extension of this ligand motif using 1,3,5-tris(4-(4-ethynylbenzonitrile)phenyl)benzene and AgOTf generates a (6,3) net.[26] A comparison of the lengths from the center of 1,3,5-tris(4-(4-ethynylbenzonitrile)phenyl)-benzene and [Co(4-papyrdpm)$_3$] to the peripherial donor atoms in these systems shows that they are very similar (Figure 7) at ∼15.0 Å[26] and ∼14.4 Å, respectively. The results presented here show that a rationally designed metalloligand, with donor atoms and structural parameters similar to those of known organic MOF building blocks, can be used to reliably form heterometallic MOFs of predictable structure. These findings demonstrate that extension of the ligand structure overrides the anion templating effect and can be used as a second means to effect dependable structural control. Because of the large number of organic ligand-derived MOFs, our findings suggest that a large number of heterometallic, and potentially functional MOFs, can be prepared with foreseeable topologies.

Thermal Analysis. Thermogravimetric analysis (TGA) of several of the evacuated frameworks showed the compounds were quite thermally stable. None of the frameworks tested displayed any significant weight loss below 200 °C (Table S1). Indeed, the average temperature at which a 5% weight loss was observed across all nine frameworks tested was 262 °C. Above 400 °C more significant losses were observed, from 25 to 80%, depending on the MOF under examination. As further evidence that the topology and hence the physical behavior of the frameworks are independent of the metalloligand metal ion, it was observed that MOF-M/AgX-1 frameworks had similar TGA profiles. For example, the TGA traces of MOF-Co/AgOTf-1 and MOF-CoFe/AgOTf-1 are very similar, whereas those of MOF-Co/AgPF$_6$-1 and MOF-Fe/AgPF$_6$-1 are comparable (Figure S5). This supports our proposition that the metalloligand metal ion can add new chemical and electronic properties to the MOF without altering the physical robustness of the network.

Conclusions

The findings reported here demonstrate that judicious metalloligand design can result in the construction of predictable

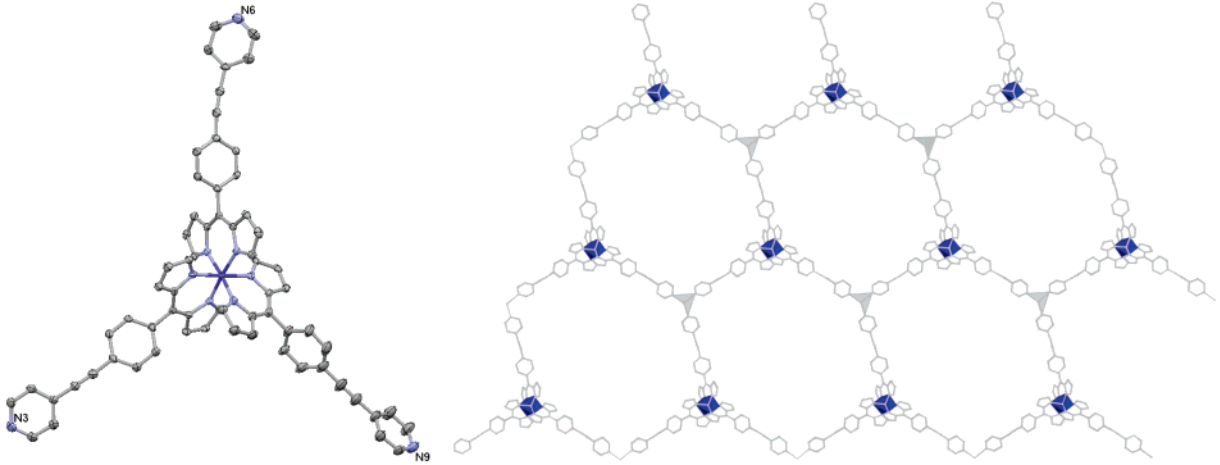

Figure 6. Structural diagram of [Co(4-papyrdpm)$_3$] (left) with partial atom numbering scheme (ORTEP, 50% probability ellipsoids). X-ray structure of the (6,3) net MOF-Co/AgPF$_6$-4 (right) viewed to highlight the (6,3) net topology. Cobalt(III) and silver(I) centers are represented by blue and gray polyhedra, respectively. Hydrogen atoms, anions, and solvent molecules have been omitted for clarity.

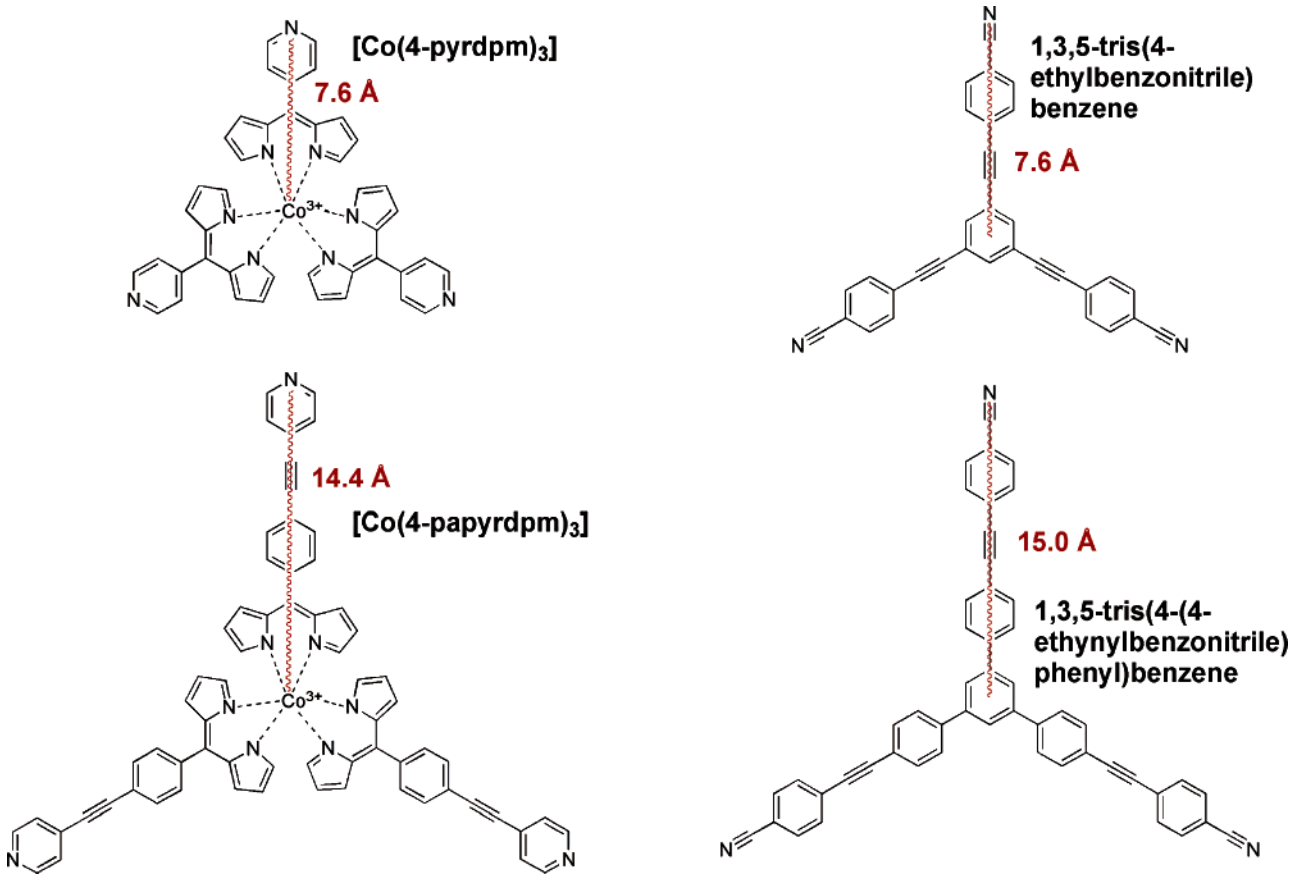

Figure 7. Comparison of the metalloligand/ligand length in [Co(4-papyrdpm)$_3$] and 1,3,5-tris(4-(4-ethynylbenzonitrile)phenyl)benzene. The red, wavy lines indicate the lengths measured.

framework structures that possess augmented physical properties. The approach is modular as demonstrated by the preparation of both iron(III) and cobalt(III) MOFs and of MOFs that contain three metal ions (Co/Fe/Ag). The experiments described provide a conceptual and synthetic strategy for the construction of a wide range of new MOFs. Both ligand design and anion templating are shown to be useful tools in controlling network topology. Experiments indicate that some of the MOFs presented are stable and can perform guest exchange with preservation of the originally templated MOF topology. Prediction of the MOF architecture based on these metalloligands can be obtained by comparison to MOFs based on analogous organic ligands already reported in the literature.

It is clear from the series of MOFs constructed in this study that the selection of silver(I) salts is crucial to the topological arrangement of some metalloligands in the final MOF. Anion templating is found to play a significant role in the assembly of these MOFs, and the templated structure is robust to anion exchange in some cases. Understanding the templating effect of these anionic species can be considered by a careful assessment of the X-ray crystallographic data of the MOFs, as well as by anion-exchange studies. Networks prepared from [M(4-pyrdpm)$_3$] and AgOTf or $AgBF_4$ yielded 3D (10,3) nets, whereas those formed from $AgPF_6$ or $AgSbF_6$ gave 2D (6,3) nets. The difference in net topology could be a kinetic effect, e.g., the PF_6^- or SbF_6^- anions "trap" an intermediate (6,3) net by a change in MOF solubility. Alternatively, the observed topologies may be due to thermodynamic differences, that is, the presence of the PF_6^- or SbF_6^- anions results in the (6,3) net being more stable relative to the (10,3) net.[42]

Whether the observed templating is kinetic or thermodynamic in origin, it is of interest to identify what features of the anion are generating this templating phenomenon. The observation that AgOTf (strongly coordinating) and $AgBF_4$ (weakly coordinating) precursors yielded similar nets indicates that coordinative ability of the anion does not play a significant role in the anion templating effect. This is further supported by a computational study of fluorinated anions, which evaluated partial charges on several species, and ranked the coordinative ability of BF_4^- lower than PF_6^- or SbF_6^-.[51] Another possible source of the templating effect might be the larger size of the PF_6^- and SbF_6^- anions. While many reports demonstrate that the shape and size of the anion can direct the assembly of supramolecular structures,[52] this does not appear to be the exclusive driving force in the systems presented here. The observation that the larger metalloligand [Co(4-papyrdpm)$_3$] overrides the anion templating effect (consistent with the analogous organic system) to generate exclusive (6,3) nets is suggestive of an effect due to size (volume) of the anion. However, substitution of OTf^- (MOF-Co/AgOTf-1) by PF_6^- in MOF-Co/Ag×PF_6-1 shows that the (10,3) nets can accommodate the larger anion, indicating that differences in anion size alone are not sufficient to explain the templating effect. An additional possibility is that the hydrogen-bonding propensity of the anion causes the observed templating effect.[52−56] There

(51) Krossing, I.; Raabe, I. *Chem. Eur. J.* **2004**, *10*, 5017−5030.
(52) Vilar, R. *Angew. Chem. Int. Ed.* **2003**, *42*, 1460−1477.
(53) Grepioni, F.; Cojazzi, G.; Draper, S. M.; Scully, N.; Braga, D. *Organometallics* **1998**, *17*, 296−307.
(54) Paul, R. L.; Z. R., B.; Jeffery, J. C.; McCleverty, J. A.; Ward, M. D. *Proc. Natl. Acad. Sci. U.S.A* **2002**, *99*, 4883−4888.

are some C−H···F contacts in the structures of MOF-M/$AgPF_6$-1 and MOF-M/$AgSbF_6$-1 that are consistent with this hypothesis (Figure S6), although we do not have sufficient data at this stage to evaluate the importance of a hydrogen-bonding contribution. It is likely that a combination of parameters (such as hydrogen bonding and, to a lesser extent, size) leads to the observed structural variations. Ongoing studies in our laboratory will help to further elucidate the role of the anions in the formation of these and related MOFs.

Acknowledgment. We thank Prof. Arnold L. Rheingold (U.C.S.D.) for help with the X-ray structure determinations, Dr. Yongshan Su for performing the mass spectrometry experiments, Prof. Clifford P. Kubiak and Prof. David N. Hendrickson for use of their FT-IR instruments. This work was supported by the University of California, San Diego, a Chris and Warren Hellman Faculty Scholar award, and the donors of the American Chemical Society Petroleum Research Fund, and the National Science Foundation (CHE-0546531 and a Graduate Research Fellowship to S.R.H.). S.M.C. is a Cottrell Scholar of the Research Corporation. Crystallographic details are available at http://www.ccdc.cam.ac.uk. Refer to CCDC reference numbers 611122, 611123, 611124, 611125, 611126, 611127, 611128, 611129, 611130, 611131, 611132, 611133, 611134, 611135, 611136, 611137, and 611138.

Supporting Information Available: Details of X-ray crystallographic analyses, Scheme S1, Figures S1−S6, and Tables S1−S3; X-ray crystallographic files in CIF format. This material is available free of charge via the Internet at http://pubs.acs.org.

JA0645483

(55) Ashton, P. R.; Cantrill, S. J.; Preece, J. A.; Stoddart, J. F.; Wang, Z.-H.; White, A. J. P.; Williams, D. J. *Org. Lett.* **1999**, *1*, 1917−1920.
(56) Campos-Fernández, C. S.; Clérac, R.; Koomen, J. M.; Russell, D. H.; Dunbar, K. R. *J. Am. Chem. Soc.* **2001**, *123*, 773−774.